



# Degradation of structural adhesive bonding joints on ship exposure decks

Hitoshi Hayashibara<sup>1</sup> · Toshiaki Iwata<sup>1</sup> · Takahiro Ando<sup>1</sup> · Chikahisa Murakami<sup>1</sup> · Eitarou Mori<sup>2</sup> · Ippei Kobayashi<sup>2</sup>

Received: 30 January 2019 / Accepted: 20 May 2019 / Published online: 4 June 2019  
© The Japan Society of Naval Architects and Ocean Engineers (JASNAOE) 2019

## Abstract

The degradation process of adhesive bonding layers on ship exposure decks was examined via an exposure test using adhesive bonding joint specimens under tensile shear load. The degradation was evaluated by the delamination and the deformation of the adhesive layer. The degradation initiated in summer, which was more significant for the specimens located at exposed areas of the ship than those in the engine room (i.e. not exposed area). Environmental measurements revealed that, in summer, the daily highest surface temperature was greatly raised at the exposed areas that, however, exhibited equal or lower average values compared to the engine room. The degradation of an adhesive bonding joint would initiate relatively rapidly in a high-temperature environment. This indicates the highest temperature is a more important factor for adhesive bonding durability than the average temperature. The tensile test conducted after the exposure test showed that the degradation progressed from the adhesive layer edge. The surface temperature on an ocean-going ship was also measured to examine the temperature condition, revealing more severe values than those on ships in mid-latitude regions such as Japan. The design temperature for adhesive bonding joints should be estimated as at least 70 °C for exposed areas.

**Keywords** Adhesive bonding joint · Degradation · Exposure deck · Surface temperature

## 1 Introduction

Using welding joints is currently the main way to build ships made of steel or other light alloy metals. Welding joints provide a ship hull and outfitting with good mechanical strength and tightness; however, the large heat input around their welding zones results in weak points since the associated structural deformations need to be corrected by additional heating after welding.

Since the mechanical properties of adhesive agents have recently been improved, the application of such materials for structural adhesive bonding joints is being extended to airplanes [1, 2], vehicles [3] and infrastructures [4]. Their application can also provide great advantages to the ship construction by reducing additional processing, such as

deformation correction or repainting of damaged coatings, because adhesive bonding does not thermally influence ship materials such as steel.

The application of adhesive bonding to ship construction has been intensively investigated during the last two decades [5–12]. The Det Norske Veritas worked on the “BONDSHIP” project, providing requirements, guidelines and examples (such as design criteria and testing method) for such use of adhesives [5, 6]. In a study conducted by The Ship’s Electric Installation Contractor’s Association of Japan, the support fittings for an electrical cable have been bonded using adhesive materials [7], while The Boat Association of Japan investigated their application to boat hulls [8]. In a previous study [9], we have demonstrated that adhesive layer will be required to be used as its thickness of millimetre order practically due to working accuracy and dimension of ship construction. We also found that, among the existing materials, the second-generation acrylic adhesive (SGA) could be the most suitable candidate for ship construction because of its relatively high strength even when used as a thick layer. In 2015, the Nippon Kaiji Kyokai published the guidelines [10] for using structural adhesives (hereafter, referred to

✉ Hitoshi Hayashibara  
hayashibara@nmri.go.jp

<sup>1</sup> National Institute of Maritime, Port and Aviation Technology, 6-38-1 Shinkawa, Mitaka-shi, Tokyo 181-0004, Japan

<sup>2</sup> National Institute of Technology, Yuge College, 1000 Shimo-Yuge, Yuge, Kamishima-cho, Ehime 794-2593, Japan

as ‘the guideline’), prescribing the approval requirements for those mainly used in the outfitting of steel and aluminium ships. These investigations [5–9] confirmed that structural adhesives can provide sufficient initial strength and work efficiency in the ship construction process. The proper design procedure and condition, such as the safety factor (SF) for adhesive strength (the guideline requires  $SF=40$ ), have been also defined [10]. Recently, FRP-metal bonded joint has been investigated for ship structure with respect to fatigue durability [11] or prediction of safety factor [12] etc.

Although long-term durability is a crucial parameter for the application of adhesive bonding joints on actual ships, only a little information is presently available about it. In a previous work, adhesive bonding joints installed in an engine room remained intact after one year of service [7], but no results were reported for a longer duration or other ship areas. Therefore, more data about the long-term durability of adhesives are required to improve the reliability of their application to ship construction.

A previous study about adhesive degradation has shown that temperature and water (moisture) are important factors affecting the durability [13]. The BONDSHIP project indicated 0–40 °C and 0–95% (relative humidity) as the minimum requirement of the environmental design conditions [5]; it also mentioned the environmental factors to be considered, but no specific value was provided. According to the guideline, an initial strength of the adhesive bonding joint in its usage environment shall be obtained in the designing process. A large temperature dependency of adhesive strength will require this provision. In such a context, the adhesive durability on a ship should be investigated by estimating the environmental conditions on it.

Estimating the adhesive durability on the exposed areas of ships is particularly urgent since, in these areas, the joints are exposed to severe conditions because of the high temperature and the presence of water (as rain, seawater and moisture). A few studies investigated the temperature on these areas: Ando et al. measured a 50–60 °C range on a floating structure in the Sea of Japan near the Yamaguchi prefecture, Japan [14], Nagano et al. recorded approximately 65 °C on the hatch cover of a ore carrier voyaging between USA and Japan [15], and Yoshikawa et al. obtained a similar value as the highest temperature on a crude oil tanker [16, 17].

In this study, the degradation process of the adhesive bonding layer on ship exposure decks was examined via an exposure test with loaded specimens and the surface temperature was measured to clarify the appropriate design conditions and promote the application of adhesive bonding joints also on such exposed areas. In addition, environmental measurements were also carried out on an ocean-going ship to obtain useful information to determine a design condition.

## 2 Experimental procedure

### 2.1 Exposure test on adhesive bonding joints

#### 2.1.1 Specimen preparation

Figure 1a illustrates the shape of the specimen used for the exposure test; the experiment was carried out on a single-lap tensile-shear joint (SLJ) because this joint type is widely used to evaluate the strength of adhesive bonding. Two aluminium alloy (JIS-H-4000, A5052) plates (63 mm length  $\times$  20 mm width  $\times$  2 mm thickness) were sandblasted and then adhesively bonded to each other so that the adhesive layer was 10 mm length  $\times$  20 mm width  $\times$   $3 \pm 0.5$  mm thickness. As mentioned above, a recent study [9] has indicated SGA as the most suitable adhesive material for ship applications; thus, a commercial SGA for structural use (C-355-20A/C-355SL-20B; Denka Co. Ltd.) was selected.

Three specimens were prepared for the initial strength test and other six for the exposure one. The former was performed on each specimen using a tensile testing machine (Autograph AG-I; Shimadzu Corp.) at room temperature (RT, 24 °C). The initial tensile shear strength ( $\tau_{ST}$ ) of the specimen adhesive bonding layer was 11.9 MPa on average (11.6, 11.7 and 12.5 MPa individually).

Six other specimens were mounted one by one on a loading jig made of stainless steel, as shown in Fig. 1b, that applied a tensile force to them via a loading spring,

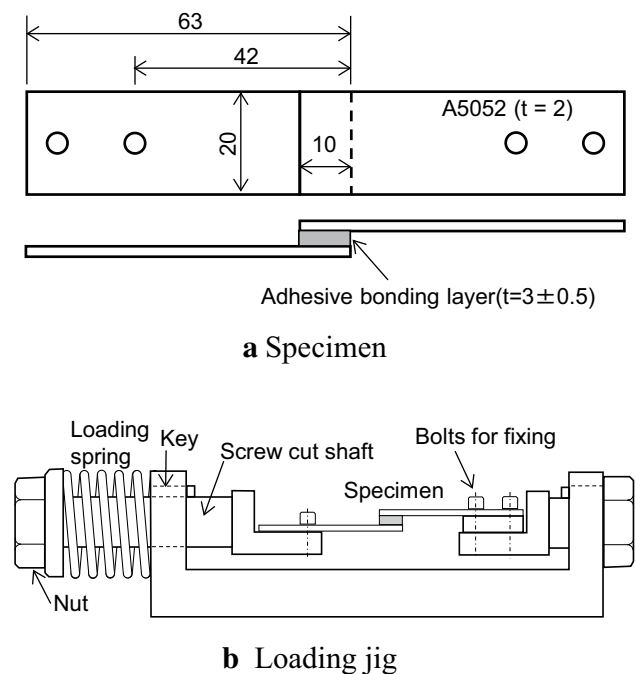


Fig. 1 Specimen and loading jig used for the exposure test

a screw-cut shaft and a nut. Using the guideline requiring an SF of 40, design strength can be calculated as 0.30 MPa (for use at RT). In the test, the exposure duration was relatively shorter than the expected service lifetime of adhesive joints on ships, but longer than other testing times previously reported. Thus, two different stress conditions, more severe than those prescribed by the guideline, were adopted to accelerate the degradation process. For the higher stress condition (HL), a tensile shear stress ( $\tau_{AP}$ ) of 3.6 MPa was applied to three specimens, with reference to the residual  $\tau_{ST}$  after the accelerating durability test required by the guideline (3.5 MPa at RT); this HL stress also corresponded to the geometrically limited value of the jig. For the lower one (LL), a stress of 2.9 MPa was applied to the other three specimens. The  $\tau_{AP}$  value was estimated and controlled by measuring the spring length since the spring constant was known (39 N/mm).

### 2.1.2 Exposure test

The exposure test was carried out from October 2015 to December 2016, for 426 days, on the training ship YUGE MARU of the National Institute of Technology, Yuge

College, which was mainly operating in the Seto Inland Sea (Japan) or moored at the college pier (Yuge Island, Japan).

The three pairs of HL and LL specimens were placed at three different locations on the ship (Fig. 2): the compass deck (CO), the starboard side of the funnel (FN) and inside the engine room (ER). Since the CO and FN locations were exposed areas, the specimens placed there directly experienced severe conditions such as sunlight irradiation, rain and wind carrying sea-salt particles, while the ER site, which was a closed space, worked as the comparison condition.

During the test, the states of the specimens were observed every few months; the  $\tau_{AP}$  of each specimen was estimated from the measured length of the loading spring and, in case of load decrease due to adhesive layer degradation, each load was corrected to its initial value by screwing the jig nut.

The environmental parameters were recorded to identify the relationship between adhesive degradation and exposure conditions. From the beginning of the test to June 2016, only the values of the surface temperature ( $T_s$ ) near the specimens were recorded via manual measurements with a surface thermometer (905-T2; Testo SE & Co.). Later, automatic measurement systems were installed on the ship to obtain more extensive data; surface temperature sensors

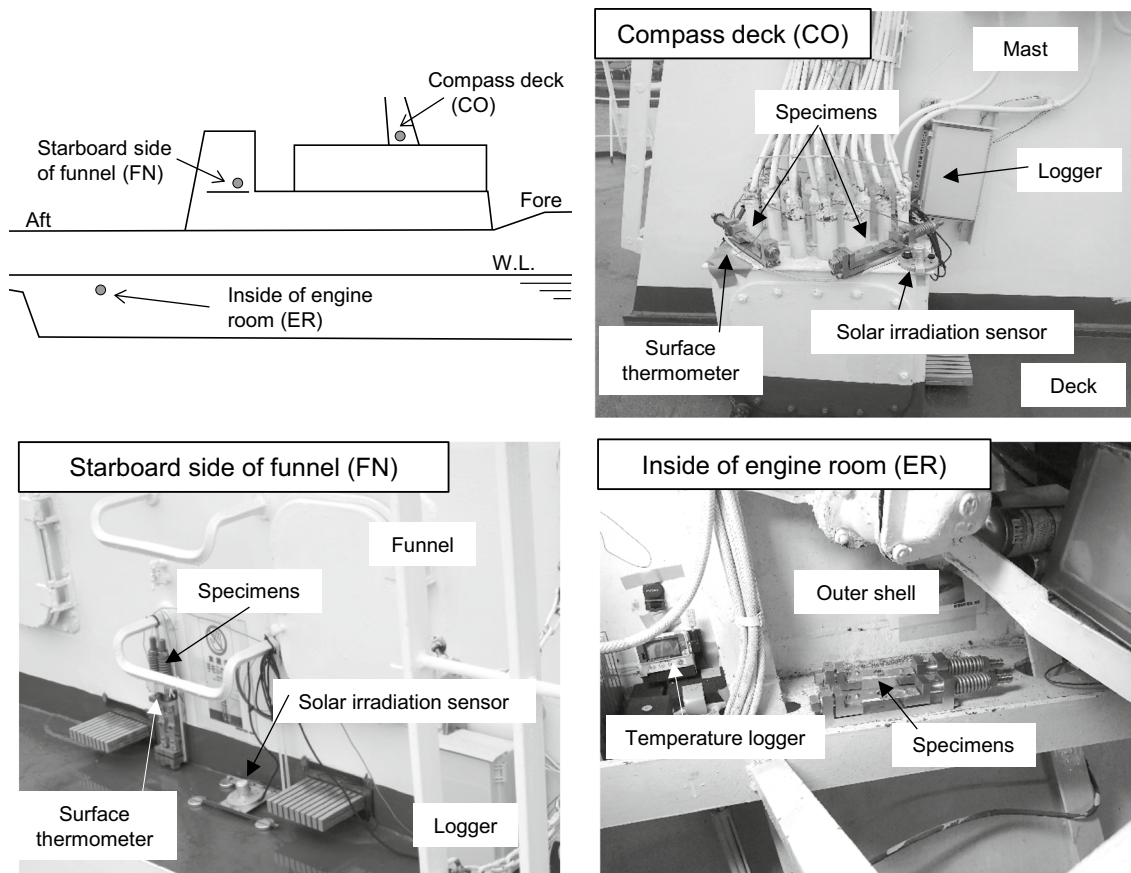


**Fig. 2** Locations of the specimens and measurement devices on the YUGE MARU ships for the exposure test

(TCKU2F; Fieldpro, Inc.) and solar radiation sensors (PCU-01B; Fieldpro, Inc.) were placed at the CO and FN locations. The sensitivity of the solar radiation sensors was in the ultraviolet (UV) range (<400 nm wavelength); hence, the total solar irradiance ( $I_{tot}$ ) was calculated from the solar irradiance measured in the UV range ( $I_{UV}$ ) using Eq. 1 and was in accordance with the solar spectrum reported by Table 4 in the CIE 085-1989 Technical Report [18]:

$$I_{tot} = \frac{I_{UV}}{0.0684} \tag{1}$$

The values measured by the sensors were recorded on data logging devices (LR5021 and LR5041; Hioki EE Corp.). In March 2016, a temperature data logger (LR5001; Hioki EE Corp.) was installed at the ER site near the specimens to record the temperature ( $T_{ER}$ ). These automatic instruments, whose arrangement is shown in Fig. 2, recorded data every 15 min.

After the exposure test, all the specimens were removed from the jig and dried in laboratory at RT. Then, the residual  $\tau_{ST}$  of each specimen was examined in the same way as for the not exposed ones.

### 2.2 Surface temperature on an ocean-going ship exposed deck

The  $T_S$  and  $I_{UV}$  values were measured also on the compass deck of a commercial cargo ship voyaging between Japan and other countries.

Figure 3 shows the schematic arrangement of the instruments used; surface thermometers were placed at four

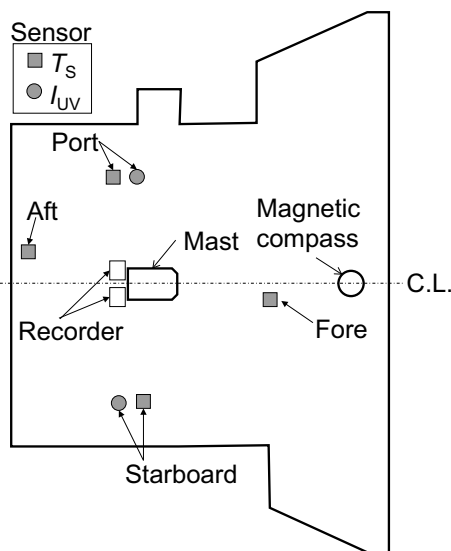


Fig. 3 Horizontal plan for the arrangement of the environmental measurement instruments on the compass deck of an ocean-going ship

locations on the deck (fore, aft, port and starboard side) and solar radiation sensors were installed on the port and starboard side, close to the thermometers. The  $T_S$  and  $I_{UV}$  values were recorded on logging instruments every 15 min, which were the same as those used on the YUGE MARU ship. The measurements were conducted for 166 days, from August 2017 to January 2018.

## 3 Results and discussion

### 3.1 Exposure test

#### 3.1.1 Adhesive bonding degradation

Figure 4 shows the relationship between testing time and specimen  $\tau_{AP}$  in the exposure test. During the first 238 days (from October 2015 to June 2016), only a little  $\tau_{AP}$  decrease was observed for the HL specimens placed at the CO and FN sites, and other specimen's  $\tau_{AP}$  did not decrease in this period, meaning that no significant degradation of the adhesive bonding layer had occurred by the 238th day (June 2016) of exposure, regardless of the stress and environmental conditions.

The tensile shear stress decreased largely during the next 83 days (from June to September 2016) of exposure in the specimens at the CO and FN sites; this decrease, together with the deformation of the adhesive bonding layer, was more evident in the HL specimens than in the LL ones. Due

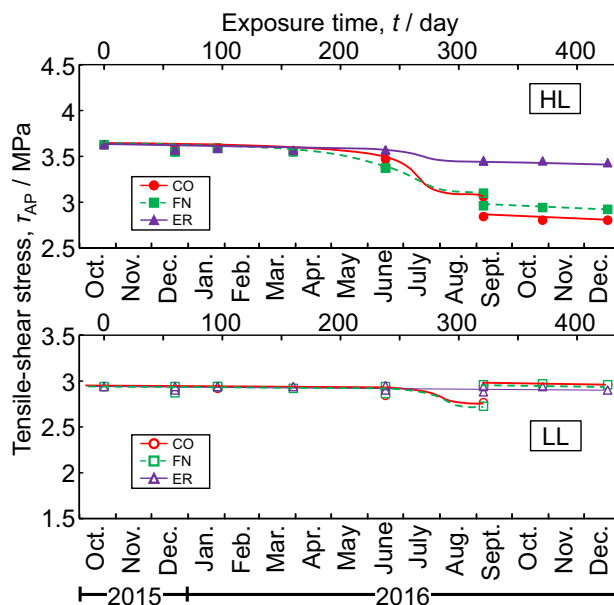


Fig. 4 Time evolution of the applied tensile shear stress  $\tau_{AP}$  of specimens of two stress conditions (HL and LL) placed on the compass deck (CO), the starboard side of the funnel (FN) and inside the engine room (ER) during the exposure test on the YUGE MARU ship



to the specimen elongation and the length constraint of the jig, the tensile load of the HL specimens in the exposed areas could not return to its initial value after the 321st day of exposure (The small sudden stress decreases of HL specimens on the CO and FN at September 2016 were not caused by the degradation or fracture of the adhesive layer. These would be due to slight unexpected rotation of the jig’s nut at the opposite side.). On the other hand, the adhesive bonding joints of both the HL and LL specimens at the ER site exhibited, respectively, only a little and no stress decrease. After the 321st day, the stress values for all the adhesive bonding joints remained stable (only a little stress decrease was observed) until the end of the exposure test, indicating that their degradation did not largely progress from September to December 2016.

Figure 5 shows the photographs of the adhesive bonding layers for the various specimens after the exposure. The bonding joints of the specimens located at CO and FN presented large deformation and delamination from the edge, while less significant changes were observed in those placed at the ER site; the delamination from the edge increased the stress level and concentration on the residual portion of the specimen, resulting in bonding layer deformation. At each exposure area, the degradation progressed more greatly in the HL specimen than in the LL one.

As a result, the degradation extent was greater at the CO and FN sites (outdoor environment) and for HL specimens than at ER and for LL ones. In addition, most of the degradation occurred between June and September 2016.

### 3.1.2 Residual strength

The residual  $\tau_{ST}$  values of the exposed specimens are tabulated in Table 1; they all exceeded the criteria recommended in the guideline (3.5 MPa). It is noted that the residual  $\tau_{ST}$  values are defined by the breaking forces of exposed

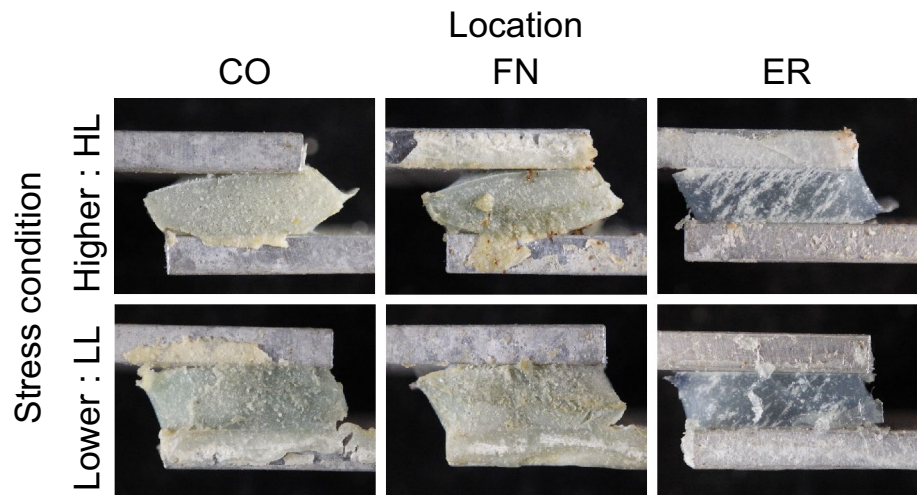
**Table 1** Tensile shear strength,  $\tau_{ST}$  values for not exposed, and exposed specimens of two stress conditions (HL and LL) placed on the compass deck (CO), the starboard side of the funnel (FN) and inside the engine room (ER), after the exposure test on the YUGE MARU ship

Specimen	$\tau_{ST}$ (MPa)
Not exposed	11.6, 11.7, 12.5
CO-HL/LL	7.3/8.8
FN-HL/LL	8.8/10.0
ER-HL/LL	11.3/12.1

specimens divided by the initial bonded area (200 mm<sup>2</sup>) when tested in RT. These  $\tau_{ST}$  were smaller after exposure at the CO and FN sites compared to those of the specimens located at ER. In the same area, larger  $\tau_{AP}$  resulted in more significant  $\tau_{ST}$  decrease, as for the more visible degradation described in Sect. 3.1.1.

The fracture surface after the tensile test consisted of three distinct areas, as shown in Fig. 6a: A, B and C. Area A was characterized by the formation of aluminium corrosion products, meaning that the adhesive layer was already delaminated in the exposure test. In area B, the adhesive layer was also completely delaminated but no corrosion product was found (the Al plate surface retained its initial state), indicating that the bonding layer already experienced degradation during the exposure and delamination in the tensile test. The residual adhesive medium observed in area C suggested that the adhesive strength value had remained relatively high there. The proportions among these three areas on each specimen were derived from the photographs. Figure 6b shows the relationship between residual strength and ratio of area C to total area ( $S_C/S_{tot}$  as area C divided by initial bonded area), including the results for the not exposed specimens; the relationship observed indicated that the residual strength was clearly correlated with  $S_C/S_{tot}$  regardless of the stress condition and exposure environment. The residual strength could be determined by  $S_C$ , meaning that the adhesive bonding in area C had not been degraded during

**Fig. 5** Photographs of the adhesive bonding layers of the specimens of two stress conditions (HL and LL) placed on the compass deck (CO), the starboard side of the funnel (FN) and inside the engine room (ER) after the exposure test on the YUGE MARU ship



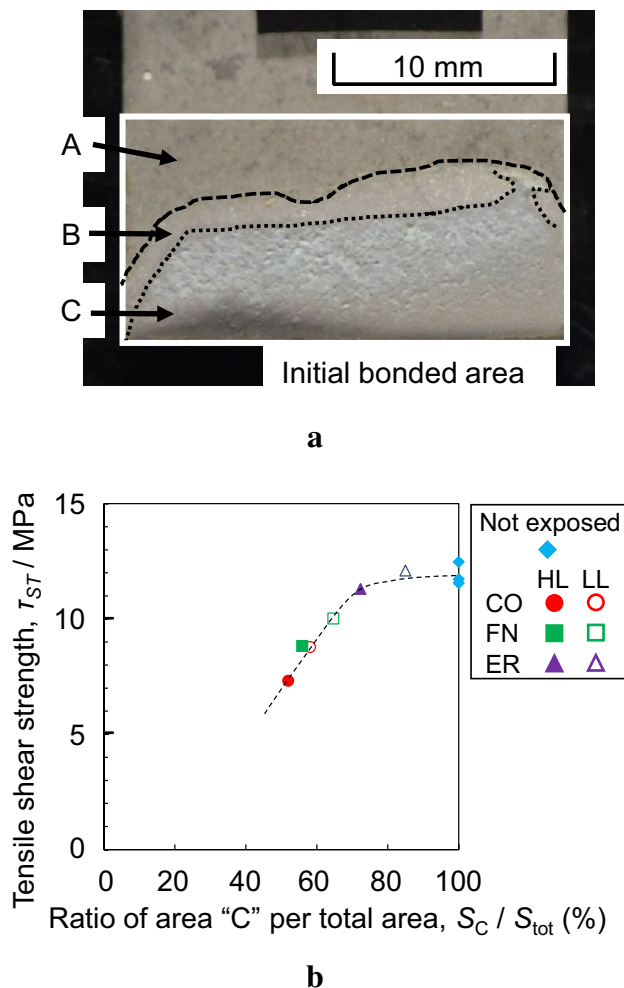


**Fig. 6** **a** Classification of the fracture surface for the specimen of HL stress condition exposed at the compass deck (CO) into area A, B and C. **b** Plots of tensile shear strength,  $\tau_{ST}$  of each specimen against ratio of area C to total area,  $S_C/S_{tot}$

more than one year of exposure to temperature changes, solar irradiation, rain and sea salt particles; in other words, the degradation progressed only from the edge of the bonding layer.

### 3.1.3 Environmental measurements

Figure 7 shows the highest, average and lowest temperature values ( $T_H$ ,  $T_{ave}$  and  $T_L$ , respectively) for each day and the cumulative solar irradiance for each month ( $I_{tot\_cum}$ ), obtained via automatic measurements. Since the manual temperature measurement was usually performed between high noon and 2 PM in a day, the resulting values ( $T_{S\_man}$ ) are also plotted with  $T_H$ . The results indicated a similarity between the CO and FN environments; in 2016,  $T_H$  for these two locations exhibited much higher values compared to the ER ones during summer (from June to early September),

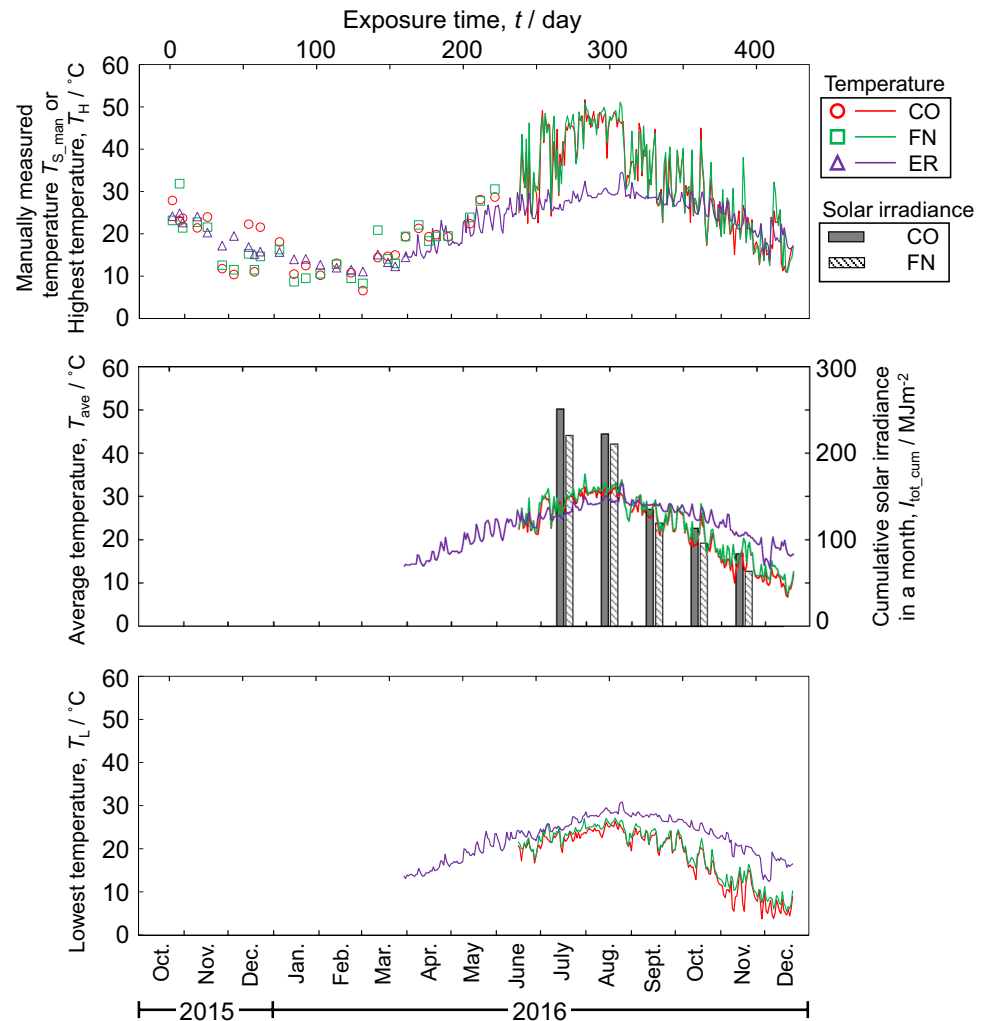
while there was a less significant difference among the three locations during the other seasons. During summer, in 2016,  $T_H$  increased up to about 50 °C at CO and FN, while no large difference was observed among the locations in terms of  $T_{ave}$ , which remained around 30 °C. From September to December 2016, ER reached higher  $T_{ave}$  than CO and FN. During summer 2016,  $I_{tot\_cum}$  exceeded 200 MJ m<sup>-2</sup> and its values were 1.6 or more times higher than those observed during the other seasons, indicating that such strong solar irradiance during summer significantly increased the  $T_H$  at CO and FN.

The highest  $T_H$  was 52 °C at CO (31 July 2016), 51 °C at FN (24 August 2016) and 35 °C at ER (25 August 2016); Fig. 8a shows, for these dates, the  $T_S$  values at CO and FN and the  $T_{ER}$  ones at ER, together with  $I_{tot}$ . A clear correlation was observed between  $T_S$  and  $I_{tot}$  at CO. These correlations are presented more clearly in Fig. 8b, showing plots of  $T_S$  against  $I_{tot}$  from 9:00 to 18:00 on 31 July 2016 for CO and 24 August 2016 for FN, respectively.  $T_S$  on CO indicated higher values for large  $I_{tot}$  values (correlation coefficient: 0.76) while  $T_S$  on FN indicated higher value against  $I_{tot} < 200 \text{ MJ}\cdot\text{m}^{-2}$  rather than against larger  $I_{tot}$  (correlation coefficient: 0.42). At FN,  $T_S$  exhibited the highest value at around 5 p.m. while the solar irradiance reached its peak between 2 p.m. and 3 p.m. This time lag could be attributed to the direction of the solar ray; as shown in Fig. 2, the specimens placed at the FN location were attached to the funnel wall, while the solar irradiance sensor faced the vertical direction so that it had poor sensitivity in the transverse direction. Since the YUGE MARU ship was always tied up, the heading direction was 206° and, hence, the specimens at FN faced to 299° direction (close to WSW). Thus, the  $T_S$  increasing around 5 p.m. was probably caused by solar irradiance from the side direction before sunset. The  $T_{ER}$  values did not change largely during the day, but they were higher than  $T_S$  at CO and FN during nighttime. This will result from that the specimens at ER did not receive any solar ray and was placed close to the ship's outer shell, whose temperature was affected by seawater rather than atmosphere. The  $T_S$  values at CO and FN were strongly affected by the solar irradiance, as reported by Ando et al. [14]; at these locations, the high solar irradiance increased  $T_S$  up to approximately 50 °C during the day, from June to September, although the corresponding  $T_{ave}$  and  $T_S$  during nighttime were equal to or less than  $T_{ER}$ .

### 3.1.4 Degradation process of the adhesive bonding layer

In view of the results from the exposure test and the environmental measurements, the degradation process of the adhesive layers on a ship can be schematized as shown in Fig. 9. Before exposure, a stress bias already exists due to the bending moment [19] and the residual stress in the adhesive

**Fig. 7** Manually measured ( $T_{S\_man}$ ), highest ( $T_H$ ), average ( $T_{ave}$ ) and lowest ( $T_L$ ) temperature values and cumulative solar irradiance ( $I_{tot\_cum}$ ) on the compass deck (CO), the starboard side of the funnel (FN) and inside the engine room (ER) during the exposure test



bonding layer. Such residual stress comes from the volume change in the adhesive media during the hardening process and the stress bias magnitude is larger in a thicker adhesive layer [20]. Hence, the initial stress profile can be drawn as shown in Fig. 9a. The stress at one edge of the adhesive layer results in the highest value in the stress profile (solid line); at this stage, layer delamination or deformation has not occurred yet since the adhesive strength (dotted line) is still enough high ( $> 11$  MPa). In the early stage of exposure (Fig. 9a), the strength value remains in an adequate state to prevent degradation, although it could be slightly decreased by heating from atmosphere and solar irradiation.

Initial (not exposed)  $\tau_{ST}$  was tested in only RT in this research. Instead, strength decrease by temperature can be predicted from the catalog data by the manufacturer [21]. For example, according to that, the strength at 30, 40 and 50 °C are expected as approximately 90%, 75% and 60% of that at 24 °C (11, 9 and 7 MPa), respectively.  $T_{S\_man}$ ,  $T_H$  and  $T_{ave}$  were translated to joint strengths at specific temperatures,  $\tau_{ST\_calc}(T_{S\_man})$ ,  $\tau_{ST\_calc}(T_H)$  and  $\tau_{ST\_calc}(T_{ave})$  using

such relation, and these are plotted against the exposure time in Fig. 10 with  $\tau_{AP}$  of HL specimens. Degradations of the specimens significantly progressed on CO and FN in the period when  $\tau_{ST\_calc}(T_H)$  on CO and FN decreased largely, while  $\tau_{ST\_calc}(T_{ave})$  did not drop so much even in summer. The nominal  $\tau_{AP}$  remained higher value than  $\tau_{ST\_calc}(T_H)$ . However, given that higher applied stress is predicted at the edge of bonding layer, stresses on such part would fall under the specific value so that delamination would start there while the residual part would retain enough strength due to the lower local stress applied, even in a high-temperature environment, as illustrated in Fig. 9b.

HL specimens would undergo larger delamination due to the larger high-stress area in the layer compared to the LL ones. As described in Sect. 3.1.3, the specimens exposed at CO and FN experienced high temperatures for a limited time each day since  $T_S$  during nighttime fell below  $T_{ER}$ , meaning that the degradation process of specimens at CO and FN progressed relatively rapidly. This could explain why the degradation observed at CO and FN was

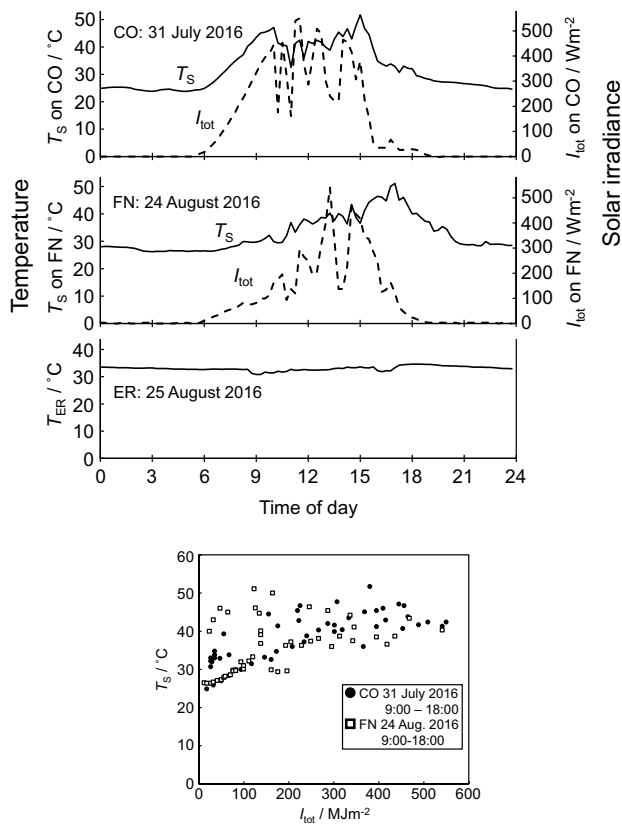


**Fig. 8** a Surface temperature,  $T_S$  and total solar irradiance  $I_{tot}$  on the compass deck (CO) and the starboard side of the funnel (FN) and temperature inside the engine room (ER,  $T_{ER}$ ), during the day when the highest temperature was recorded at each location. b Plots of  $T_S$  against  $I_{tot}$  from 9:00 to 18:00, on 31 July 2016 for CO and 24 August 2016 for FN

more significant than that at ER while the latter location exhibited  $T_{ave}$  values equal to or higher than those for the other two.

Such high  $T_H$  environment also might introduce heat cycle fatigue on the adhesive layer. However, degradation was significant only during summer while heat cycle can be caused by not only rising  $T_H$  (summer) but also  $T_L$  descending (winter). This means that the highest temperature in itself, reached in the usage environment is more important than the average temperature or the difference

between highest and lowest temperature (heat cycle) when designing an adhesive bonding joint.

Larger peel stress is expected on the edge of bonding layer of the tested specimens than that of actual structure since thin plates were used for the specimen’s base metal. Such peel stresses will enhance delamination from the edge. Thus this research can not provide the design criteria such as safety factor or threshold load value for long time use. However, actual bonding joints on more rigid bases eventually have a certain degree stress concentration on its edge. Thus, paying attention to highest temperature will also be important environmental information for actual structures constructed with adhesive bonding joints.

The layer delamination would gradually spread from its edge as described in Sect. 3.1.2. It will be associated with gradual  $\tau_{AP}$  decrease observed from September to December 2016 as shown in Fig. 4. Such gradual degradation had proceeded more slowly than rapid degradation in summer, which might be influenced by water absorption from moisture, rain or sea water, in low temperature environment after September 2016, as drawn in Fig. 9c. There is no additional experiment in this research. However, in general, water absorption causes bonding layer degradation [13]. We previously confirmed the influence of moisture on the SGA adhesion tested in this research by acceleration tests [22]. The delamination-shaped crevice boundaries of the adhesive layer would facilitate this process by interrupting water drying from its boundaries. Preventing water (or other degradation factors if they are important) ingress might be effective to ensure long-term durability of adhesive bonding joints though the quantitative effect of water on long term exposure should be examined by the additional test thoroughly.

### 3.2 Surface temperature on the exposed deck of an ocean-going ship

The  $T_H$  values and  $I_{tot\_cum}$  observed on the ocean-going ship are shown in Fig. 11, revealing a wider  $T_H$  range than that observed on the YUGE MARU, probably due to the larger environmental variety where the ocean-going ship was navigated. The highest  $T_H$  was 75 °C on the fore (24 September 2017), 71 °C on the starboard side (21 August 2017), 70 °C on the port side (24 September 2017) and 78 °C on the aft

**Fig. 9** Schematic of the degradation process of an adhesive bonding layer exposed on a ship deck

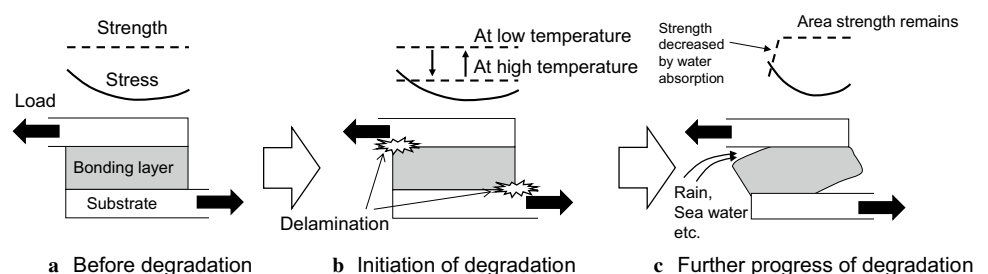




**Fig. 10** Plots of predicted strength for specific temperature based on catalog data at  $T_{man}$ ,  $T_H$  and  $T_{ave}$ , with  $\tau_{AP}$ , against the exposure time

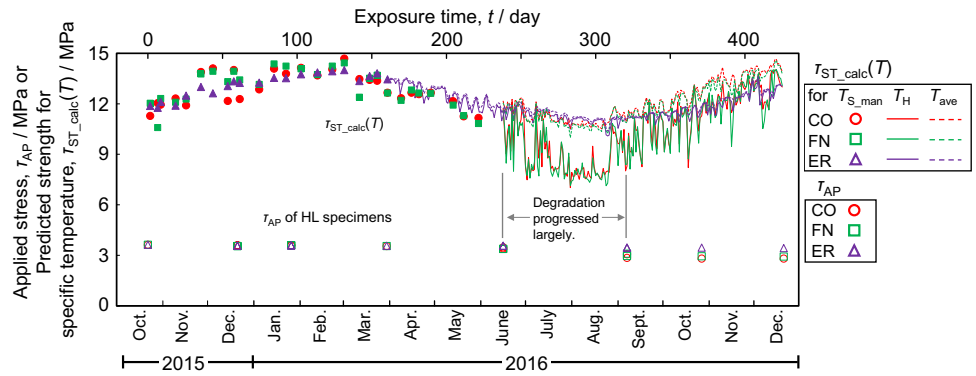


**Fig. 11** Highest temperature,  $T_H$  and cumulative solar irradiance,  $I_{tot\_cum}$  for each month on the compass deck of an ocean-going ship

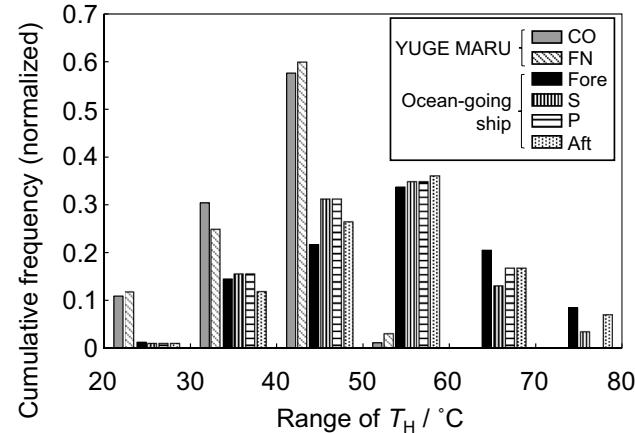
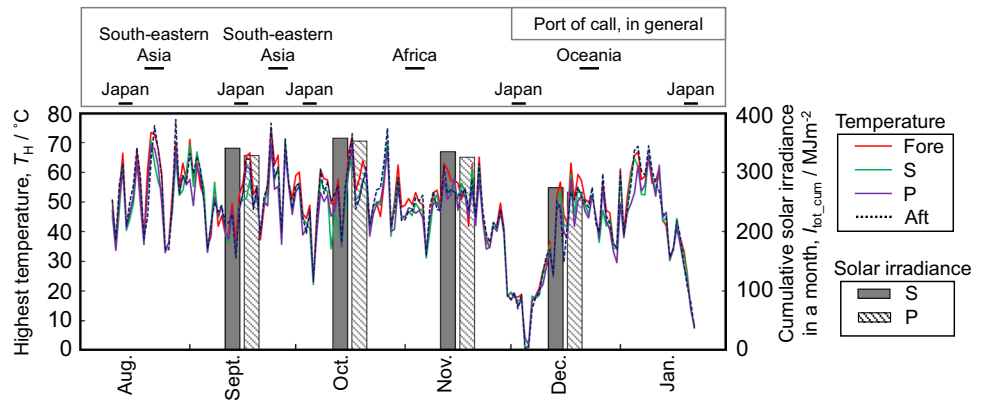


**Fig. 12** Cumulative frequency of the highest temperature,  $T_H$  on the YUGE MARU (from July to September 2016) and an ocean-going ship (from August to October 2017)

(28 August 2017); these values were slightly higher than those reported in literature [15–17]. In addition,  $I_{tot\_cum}$  was always larger compared to the YUGE MARU case. Figure 12 compares the  $T_H$  values measured on the YUGE MARU (from July to September 2016) and on the ocean-going ship (from August to October 2017), clearly indicated that the temperature on the latter was much severe than on

the former. On the ocean-going ship,  $T_H$  exceeded 70 °C on several days and, according to the information about the ports of call, such high values were usually recorded at low-latitude regions, where the atmospheric temperature tends to be higher compared to mid-altitude regions such as the Seto Inland Sea. The large  $T_H$  on the ocean-going ship could be attributed to a combined effect of high atmospheric temperature and large solar irradiance at low-altitude regions. Hence, although these data were obtained for only one ship in this study, a design temperature of at least 70 °C should be considered for adhesive bonding joints on exposed areas of ocean-going ships.

### 4 Conclusions

The degradation process of adhesive bonding joints on ship exposure decks was investigated via an exposure test on an actual ship, including environmental measurements and residual strength evaluation; in addition, the surface temperature was also measured on an ocean-going ship. The following conclusions could be drawn.

1. The highest temperature in a day, rather than the average temperature, is an important factor for an adhesive

bonding joint design ensuring durability for use on a ship exposure deck.

2. To ensure the long-term durability of adhesive bonding joints on ship exposure decks, their shape should prevent to exclude degradation factors such as water from the adhesive/substrate interface since the degradation progresses from the joint edge.
3. A design temperature of at least 70 °C should be considered for adhesive bonding joints to be used on exposed areas of ocean-going ships.

**Acknowledgements** Capt. Nagamoto of YUGE MARU, Mr. Akiyama and Dr. Yamane of NMRI assisted to carry out the exposure test on YUGE MARU. Ocean Trans Co., Ltd. And NIPPON KAIJI KYOKAI (Class NK) also arranged the measurements on the ocean-going ship. The authors are grateful to these cooperation.

## References

1. Yamamoto T (2001) Application of adhesive bonded structure for air and space vehicle. *J Jpn Weld Soc* 70:24–27
2. Seneviratne W, Tomblin J, Kittur M (2015) Durability and residual strength of adhesively-bonded composite joints: the case of F/A-18 A-D wing root stepped-lap joint, fatigue fracture of adhesively-bonded composite joints. Elsevier, Amsterdam, pp 289–320
3. Zhang F, Yang X, Wang HP, Zhang X, Xia Y, Zhou Q (2013) Durability of adhesively-bonded single lap-shear joints in accelerated hygrothermal exposure for automotive applications. *Int J Adhes Adhes* 44:130–137
4. Sousa JM, Correia JR, Fonseca SC (2018) Some permanent effects of hygrothermal and outdoor ageing on a structural polyurethane adhesive used in civil engineering applications. *Int J Adhes Adhes* 84:406–419
5. Weitzenböck JR (2005) BONDSHIP project guidelines. Det Norske Veritas, Dag McGeorge
6. Roland F, Manzon L, Kujala P, Brede M, Weitzenböck J (2004) Advanced joining techniques in shipbuilding. *J Ship Prod* 20:200–210
7. The Ship's Electric Installation Contractor's Association of Japan (2006) Research report of new installation working of electric equipment by adhesive materials
8. Miyairi H (2010) Development of boat construction technology by using structural adhesive. *Shutei Giho (Boat Eng)* 103:2–6
9. Akiyama S, Iwata T, Shimada M, Ando T, Murakami C, Anai Y, Hayashibara H, Tanaka Y (2012) Research study of outfitting technology applied adhesive. *Pap Natl Marit Res Inst* 12:17–39
10. NIPPON KAIJI KYOKAI (Class NK) (2015) Guidelines for use of structural adhesives, 1st edn. Class NK, Tokyo
11. Boyd W, Blake JIR, Sheno RA, Kapadia A (2004) Integrity of hybrid steel-to-composite joints for marine application. *J Eng Marit Environ* 128:235–246
12. Ritter GW, Speth DR, Yang YP (2009) Qualifications of adhesives for marine composite-to-steel bonded applications. *J Ship Prod* 25:198–205
13. Costa M, Viana G, da Silva LFM, Campilho RDSG (2017) Environmental effect on the fatigue degradation of adhesive joints: a review. *J Adhes* 93:127–146
14. Ando S, Hoshino K, Yamagishi N (1990) The field tests of prototype floating offshore structure part 2. On the distribution of temperature by solar radiation for experimental structure. *J Soc Nav Arch Jpn* 167:301–311
15. Nagano K, Sakata H, Yoshikai K, Handa K (1986) A consideration on the design of long hatch cover. *J Seibu Zosen Kai* 71:221–231
16. Yoshikawa M (2004) Corrosion of cargo oil tanks of VLCC tankers. *Zairyo-to-Kankyo* 53:388–395
17. Soares CG, Garbatov Y, Zayed A, Wang G (2008) Corrosion wastage model for ship crude oil tanks. *Corros Sci* 50:3095–3106
18. International Commission on Illumination (1996) Solar spectral irradiance. Technical report CIE 085-1989, 1996
19. Goland M, Buffalo NY, Reissener E (1944) The stresses in cemented joints. *J Appl Mech* 11:17–27
20. Okubo K (2004) Adhesive evaluation by finite element method. *Technol Adhes* 75:73–76
21. Denka Co. Ltd.: HARDLOC Brochure (sheet metal). <https://www.denka.co.jp/eng/pdf/product/detail/00029/HARDLOC%20Brochure%20%28Sheet%20metal%29%20%28JAPANESE%20ONL%29.pdf>. Accessed 15 Apr 2019
22. Iwata T, Hayashibara H (2019) Durability and flammability evaluation of SGA structural adhesives joint consisting of thick adhesive layer for shipbuilding. *J Adhes* 95:614–631

**Publisher's Note** Springer Nature remains neutral with regard to jurisdictional claims in published maps and institutional affiliations.